

5G HAIRPIN BANDPASS FILTER

Sahar Saleh¹, Widad Ismail¹, Intan Sorfina Zainal Abidin¹, Mohd Haizal Jamaluddin²,
Mohammed H. Bataineh³ and Asem S. Alzoubi³

(Received: 15-Aug.-2020, Revised: 28-Sep.-2020, Accepted: 13-Oct.-2020)

ABSTRACT

In this paper, Hairpin Bandpass Filter (HPBF) is designed, simulated and fabricated at two 5G low-frequency bands: 3.7 GHz - 4.2 GHz and 5.975 GHz - 7.125 GHz. This filter will be a part of our 5G narrowband/ Ultra Wide Band (UWB) reconfigurable antenna project that plays a significant role in the recent wireless networks, such as Cognitive Radios (CRs). Through the two frequency bands, the filter resulted in good matching and transmission responses with enhanced bandwidth. The measured reflection coefficient of the proposed HPBF, S_{11} is < -10 dB and < -11.66 dB through 3.45 GHz – 4.25 GHz and 5.62 GHz – 7.6 GHz, respectively. However, the transmission coefficient, S_{12} is around -1.5 dB and -1.17 dB at the center frequencies $F_C = 3.75$ GHz and 6.61 GHz, respectively. In this paper, the High-Frequency Structure Simulator (HFSS) software is used to carry out the simulation. The full-wave simulation results are validated with the hardware measurements.

KEYWORDS

Hairpin bandpass filter (HPBF), Harmonics suppression, 5G, Reconfigurable antenna, Cognitive radios (CRs), HFSS.

1. INTRODUCTION

Filters play an important role in many RF/Microwave applications and are used to control the frequency responses (band-pass, band-stop, low-pass and high-pass) to overcome the limitation of the electromagnetic spectrum and facilitate the possibility to share it. HPBF is a compact structure bandpass filter which is simply constructed by folding the $\lambda/2$ resonators of the parallel-coupled filter, to get the U shape that eases its fabrication process, where no grounding *via* holes is needed [1]. HPBF has been recently used in many applications at different frequencies, such as Ku-band satellite communication [2]-[3], WiMAX [4]-[5], Wireless Local Area Network (WLAN) [6] and millimeter-wave applications [7]-[8]. In [9], X- band 9.3 GHz HPBF with a bandwidth (BW) of 0.28 GHz was designed for radar navigation; however, a 2 GHz – 4 GHz HPBF was designed in [10] for satellite application. For the 5th generation mobile communication system, authors in [11] designed three different 20 GHz HPBFs with different feeding techniques. It was found that the filter with input/output feed structure is better than the one with tap-type feed in terms of insertion and return losses. Authors in [12] designed HPBF with sharp frequency response suitable for narrowband communication, such as the uplink frequency in the band -3 eNodeB LTE (1.710 GHz-1.785 GHz). A 6-order unlicensed frequency band (2.2 GHz to 2.3 GHz) HPBF that meets electromagnetic interference (EMI) or electromagnetic compatibility (EMC) issues requirements was designed in [13]. In [14], the authors designed HPBF for 923 MHz RFID application. Second harmonics suppression for 1 GHz HPBF was achieved using modified Minkowski fractal shape in [15]. Besides, Defected Ground and Microstrip Structures (DGS) and (DMS) were used in HPBF for performance enhancement and size reduction. Superior harmonics suppression in the response of HPBF is obtained in [16] by adding different DMSs to the filter's resonators. The resulted suppressions were -25 dB and -40 dB for the second and the third harmonics, respectively. In [17], dumbbell-shaped DGS cells are etched at the input and output ports of a five-pole 2.5 GHz HPBF to enhance high-order harmonics suppressions. Extra harmonics suppression was also achieved by introducing an open stub at the feedline of the designed filter. Authors in [18] also used two pairs of dumbbell-shaped DGS cells at the feed lines of a 3-GHz HPBF used for microwave imaging application to enhance the BW in addition to get better S_{11} . In addition, to enhance the filter response, size reduction can also be achieved by adding square DGSs to HPBFs used for S-band [19]-[20] and X-band radar

1. S. Saleh, W. Ismail and I. S. Z. Abidin are with School of Electrical and Electronic Engineering, Universiti Sains Malaysia, Penang, Malaysia. Emails: sahar_saleh@student.usm.my, eewidad@usm.my and intan.sorfina@usm.my

2. M. H. Jamaliddin is with Wireless Communication Centre, Universiti Teknologi Malaysia, Johor, Malaysia. Email: haizal@utm.my

3. M. Bataineh and A. Alzoubi are with Hijjwai Faculty for Engineering Technology, Yarmouk University, Irbid, Jordan. Emails: mohbat@yu.edu.jo and asem@yu.edu.jo

applications [21]. However, in [22], dumbbell and stepped hairpin resonator (SHPR) DGS shapes are used for second harmonics suppression below -30 dB for a 2.4-GHz HPBF with 29% FBW. The design in [19] was enhanced using the dumbbell DGS [23]. Tapped feed lines are also used for harmonics suppression as in [24] by controlling the two transmission zeros. The designed 8.75-GHz HPBF provided 1 to 8 GHz and 9 to 15 GHz harmonics suppression. Furthermore, Plackett-Burman Design of Experiment methodology (DOE) was applied in designing a 2.4-GHz HPBF for further optimization. Resulted insertion and return loss of this filter were improved by 61% and 15 % from the designed one with Gensys software [25]. Many techniques were developed to reduce the size of HPBF, such as adding ground holes, a high dielectric substrate, multilayer structure, nonuniform coupled line resonators, aperture coupled line resonators, metamaterial complementary split ring resonators, Inkjet Printing and integrated passive device (IPD) technologies. A 37 % of size reduction was achieved in designing a 923-MHz HPBF with 7.5 MHz BW *via* hole grounding [14]. However, an 11% size reduction with spurious harmonics suppressions was obtained for a 1-GHz HPBF in [26] using novel fractal shaped lines (FSLs). For low-cost and high-performance integrated circuits, Inkjet Printing Technology (IPT) is used in [7] to design a 30-GHz millimeter wave HPBF on Liquid Crystal Polymer (LCP) substrate. Conventional Uniform Transmission Lines (UTLs) of 2.06 GHz HPBF resonators were replaced by artificial left-handed and right-handed transmission lines (LHRHTLs) in [27] for size reduction. For further compactness, these artificial lines were implemented in the form of multilayered structures by using liquid crystal polymer technology (LCPT). Compact size with spurious harmonic response suppression was obtained by using nonuniform coupled lines (NCLs) resonators to design a 34-GHz HPBF in [8]. A five-pole ISM band HPBF with approximately 40 % size reduction was designed in [28] using two stacked microstrip layers. In this filter, two apertures are introduced in the common ground planes to provide coupling between resonators at the two layers. A high dielectric substrate (Al_2O_3 ceramic) was used to design a compact C-band HPBF in [29]. A compact HPBF with a selective 100 MHz WLAN BW was proposed in [6] using two short-circuited comb-lines coupled with a Rectangular Shaped Loop Resonator (RSLR). For the first time, integrated passive device (IPD) technology was used in [30] to design a compact W-band 95.5-GHz HPBF with 8 GHz BW. A GaAs substrate with a thickness of 0.100 mm and two metal layers were employed to design the filter using PID technology. In [5], a compact multi-band (3.5 GHz and 5.5 GHz) HPBF was proposed using metamaterial complementary split ring resonators. Multilayer techniques are used in [2] for significant size reduction and enhanced Ku-band HPBF performance. An HPBF with a tunable center frequency of 650 MHz to 920MHz and a BW of 25MHz and 85 MHz was designed in [31] using Screen Printed Ferroelectric Varactors. However, in [32], a barium strontium titanate (BST) thin film was used for continuous control on center frequency (from 900MHz to 1.1 GHz) and BW (from 40MHz to 80MHz) of the designed HPBF. A $\lambda/4$ stub resonator was added to the filter to increase the stop attenuation and band isolation by controlling the introduced transmission zero at the upper frequency.

5G is a revolutionary technology that aims to enhance the communication link data rate [33]-[34], reduce the latency and increase the reliability [35]-[37] to meet the growing demand of mobile users and to be suitable for (Internet of Things) IoT networking services [38]. On October 24, 2018, the Federal Communication Commission (FCC) has proposed two frequency bands below 24 GHz: licensed (C-Band: 3.7 GHz-4.2 GHz) and unlicensed (5.925 GHz -6.425 GHz, 6.525 GHz -6.875 GHz and 6.875 GHz – 7.125 GHz bands (totally 5.925 GHz–7.125 GHz)) spectrum for 5G technology [39]. In this work, as a contribution to 5G technology, an HPBF is designed at these two frequency bands a wider resulting BW as compared to other filters in the literature. For recent wireless communication system

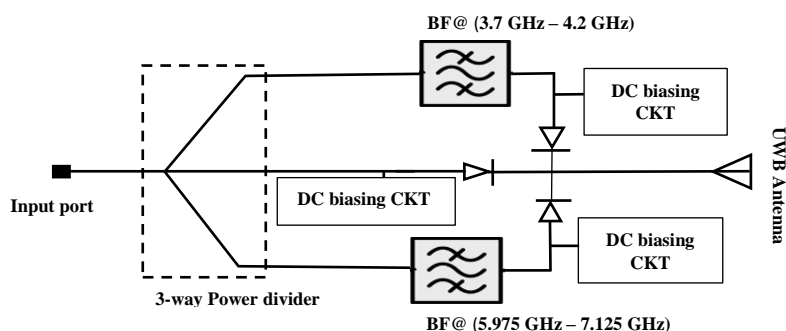


Figure 1. Future project: 5G narrowband / UWB reconfigurable antenna.

2. HAIRPIN BANDPASS FILTER

To reduce the size of the parallel-coupled $\lambda/2$ resonator filter, its resonators as shown in Figure 2a can be folded to get the U shape as in Figure 2b, forming a new type of bandpass filter called Hairpin Bandpass Filter (HPBF). In addition to HPBF compact structure, it is preferable due to its ease of fabrication, where no grounding *via* holes is needed [1].

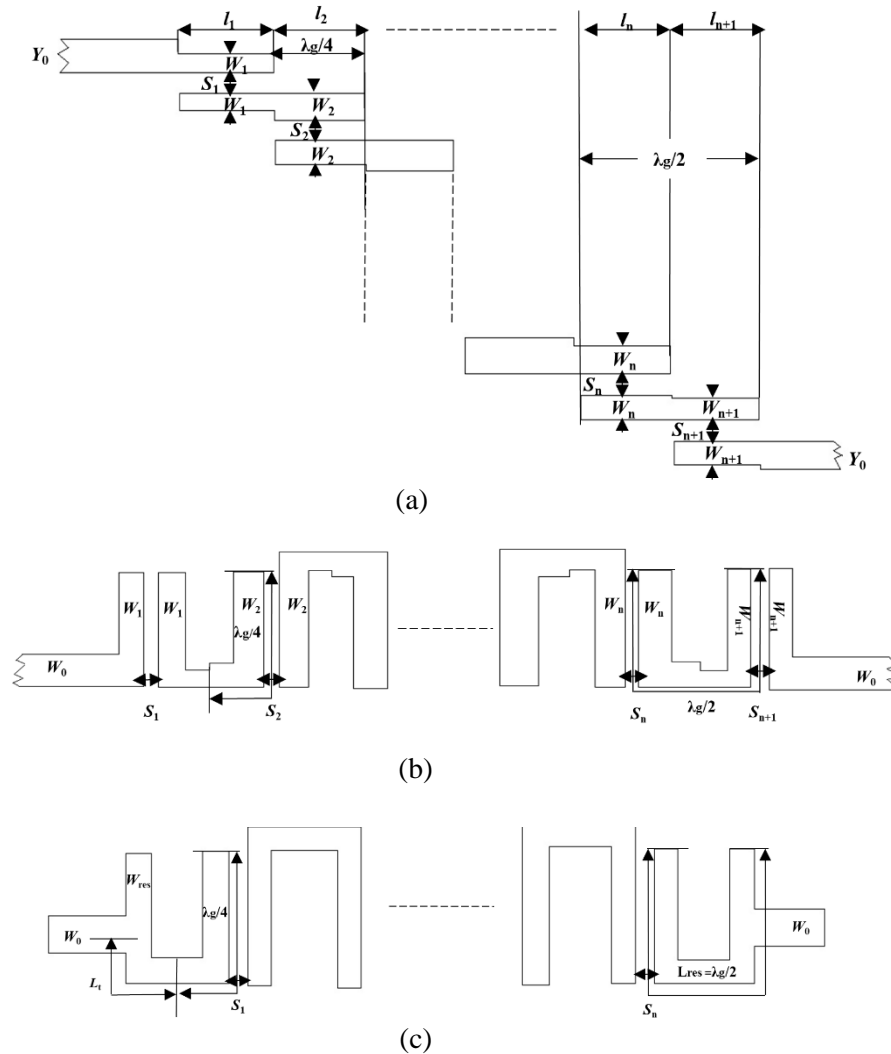


Figure 2. N-order (a) Parallel-coupled $\lambda/2$ resonator filter into (b) and (c) HPBF.

The characteristics impedance of each resonator of n^{th} -order HPBF can be found in [1]:

$$(Z_0)_{j,j+1} = \sqrt{(Z_{0e}^2)_{j,j+1} + (Z_{0o}^2)_{j,j+1}} \quad (1)$$

where

$$(Z_{0e})_{j,j+1} = \frac{1}{Y_0} \left[1 + \frac{J_{j,j+1}}{Y_0} + \left(\frac{J_{j,j+1}}{Y_0} \right)^2 \right], \quad \text{for } j = 0 \text{ to } n \quad (1.1)$$

$$(Z_{0o})_{j,j+1} = \frac{1}{Y_0} \left[1 - \frac{J_{j,j+1}}{Y_0} + \left(\frac{J_{j,j+1}}{Y_0} \right)^2 \right], \quad \text{for } j = 0 \text{ to } n \quad (1.2)$$

$$\frac{J_{01}}{Y_0} = \sqrt{\frac{\pi FBW}{2g_0g_1}}, \quad (1.3)$$

$$\frac{J_{j,j+1}}{Y_0} = \frac{\pi FBW}{2\sqrt{g_jg_{j+1}}}, \quad \text{for } j = 1 \text{ to } n-1 \quad (1.4)$$

and

$$\frac{J_{n,n+1}}{Y_0} = \sqrt{\frac{\pi FBW}{2g_n g_{n+1}}} \quad (1.5)$$

where Y_0 and $J_{j,j+1}$ are the characteristic admittances of terminating lines (input and output ports) and J inverters, respectively. $g_0, g_1 \dots g_n$ are the elements of a ladder-type lowpass prototype with a normalized cutoff, $\Omega_c = 1$ and FBW is the fractional BW of bandpass filter which is equal to:

$$FBW = \frac{F_c}{BW} \quad (1.6)$$

After calculating the characteristic impedance of each resonator in (1), its width can be calculated using an online microstrip line calculator [41] based on the following familiar microstrip line Equation [42]:

$$W = \begin{cases} \frac{8he^A}{e^{2A}-2}, & \frac{W}{h} < 2 \\ \frac{2}{\pi}h \left\{ B - 1 - \ln(2B - 1) + \frac{\epsilon_r - 1}{2\epsilon_r} \left[\ln(B - 1) + 0.39 - \frac{0.61}{\epsilon_r} \right] \right\}, & \frac{W}{h} > 2 \end{cases} \quad (2)$$

$$A = \frac{Z_0}{60} \sqrt{\frac{\epsilon_r + 1}{2}} + \frac{\epsilon_r - 1}{\epsilon_r + 1} \left(0.23 + \frac{0.11}{\epsilon_r} \right), \quad (2.1)$$

$$B = \frac{377\pi}{2Z_0\sqrt{\epsilon_r}}. \quad (2.2)$$

Two important parameters controlling the performance of the filters are the separation between the adjacent resonators, S and the tapped line at the input and at the output, L_t . Details on their effect will be addressed in the upcoming sections. S and L_t can be determined by the mutual coupling coefficient, $M_{i,i+1}$ and the external quality factor of the filter, Q_e , respectively. These design parameters are given as follows [1]:

$$Q_{e1} = \frac{g_0 g_1}{FBW}, \quad Q_{en} = \frac{g_n g_{n+1}}{FBW}, \quad M_{i,i+1} = \frac{FBW}{\sqrt{g_i g_{i+1}}}, \quad \text{for } i = 1 \text{ to } n \quad (3)$$

where Q_{e1} and Q_{en} are the input and output external quality factors.

It should be mentioned here that in Full-wave Electromagnetic simulations, such as ANSYS HFSS, the relation between S and $M_{i,i+1}$ and between L_t and Q_e can be extracted using [1]:

$$Q_e = \frac{w_0}{\Delta w \pm 90^\circ}, \quad M_{i,i+1} = \pm \frac{f_{p2}^2 - f_{p1}^2}{f_{p2}^2 + f_{p1}^2}, \quad (4)$$

where w_0 , $\Delta w \pm 90^\circ$, f_{p2} and f_{p1} are the angular center frequency, absolute BW between $\pm 90^\circ$ points, high- and low-frequency peaks, respectively.

In this study, the g 's values of Chebyshev response lowpass prototype with 0.1 dB passband ripple are $g_0 = g_4 = 1$, $g_1 = g_3 = 1.0316$, $g_2 = 1.1474$. In addition, the chosen substrate material is Rogers RO4003C with $\epsilon_r = 3.55$, height $h = 0.813$ mm and dielectric loss tangent = 0.0027.

3. 3.95-GHZ HAIRPIN BANDPASS FILTER

At $F_c = 3.95$ GHz of the 5G lower band (3.7 GHz- 4.2 GHz) and using the design Equations (1)-(4), a 3.95-GHz HPBF is designed and simulated using ANSYS HFSS. The calculated and optimized parameters are shown in Table 1, where L_{res} , W_{res} , S , L_t , L_{p1} , L_{p2} and W_p are the length of the resonator, the width of the resonator, the space between two adjacent resonators, tapping length, length of the first and second ports and width of the ports, respectively. Figures 3a and 3b show the relation between S and $M_{1,2}$ and between L_t and Q_e , respectively. The detailed parametric studies are shown in Figure 4.

Table 1. Calculated and optimized parameters of 3.95-GHz HPBF.

Parameters	Calculated	Optimized
Q_e	8.14	-
$M_{12}=M_{21}$	0.12	-
L_{res} (mm)	23.268	23
W_{res} (mm)	0.595	0.45
S (mm)	0.9	0.3
L_t (mm)	1.3	2.7
L_{p1} (mm)	-	3

L_{p2} (mm)		3
W_p (mm)	1.819	1.5

The chosen optimized values are in red color with dashed red box, which indicates the acceptable matching and the smallest ripples within and beyond the required band (3.7 GHz – 4.2 GHz), respectively. As noticed from Figure 4a, the band is shifted to the left or right as L_{res} increased or decreased, respectively. Good matching is obtained when $W_{res} = 0.45$ mm, as shown in Figure 4b. Figure 4c illustrates that to increase the BW, the coupling between resonators should be increased by decreasing S . Better matching is obtained when L_t is larger than the calculated one, as shown in Figure 4d and finally, good matching within the required band is obtained when the port width is less than 1.819 mm, as indicated in Figure 4e.

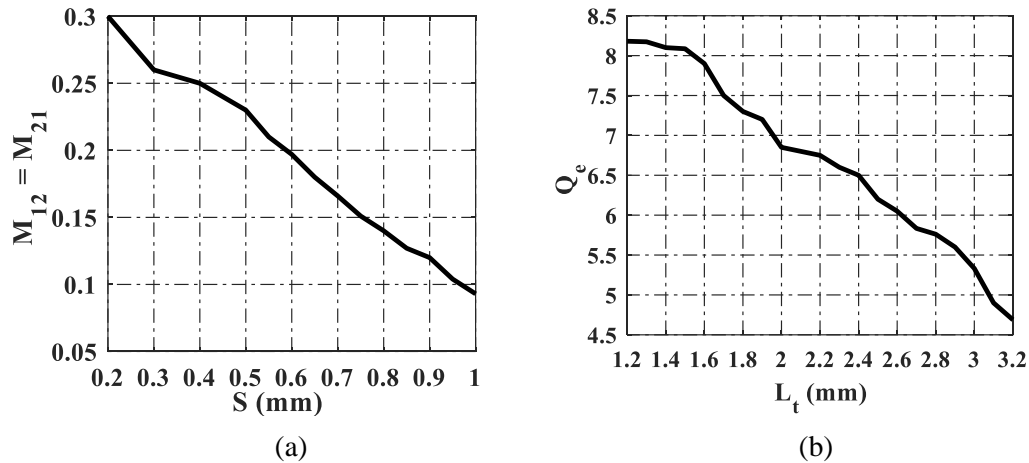
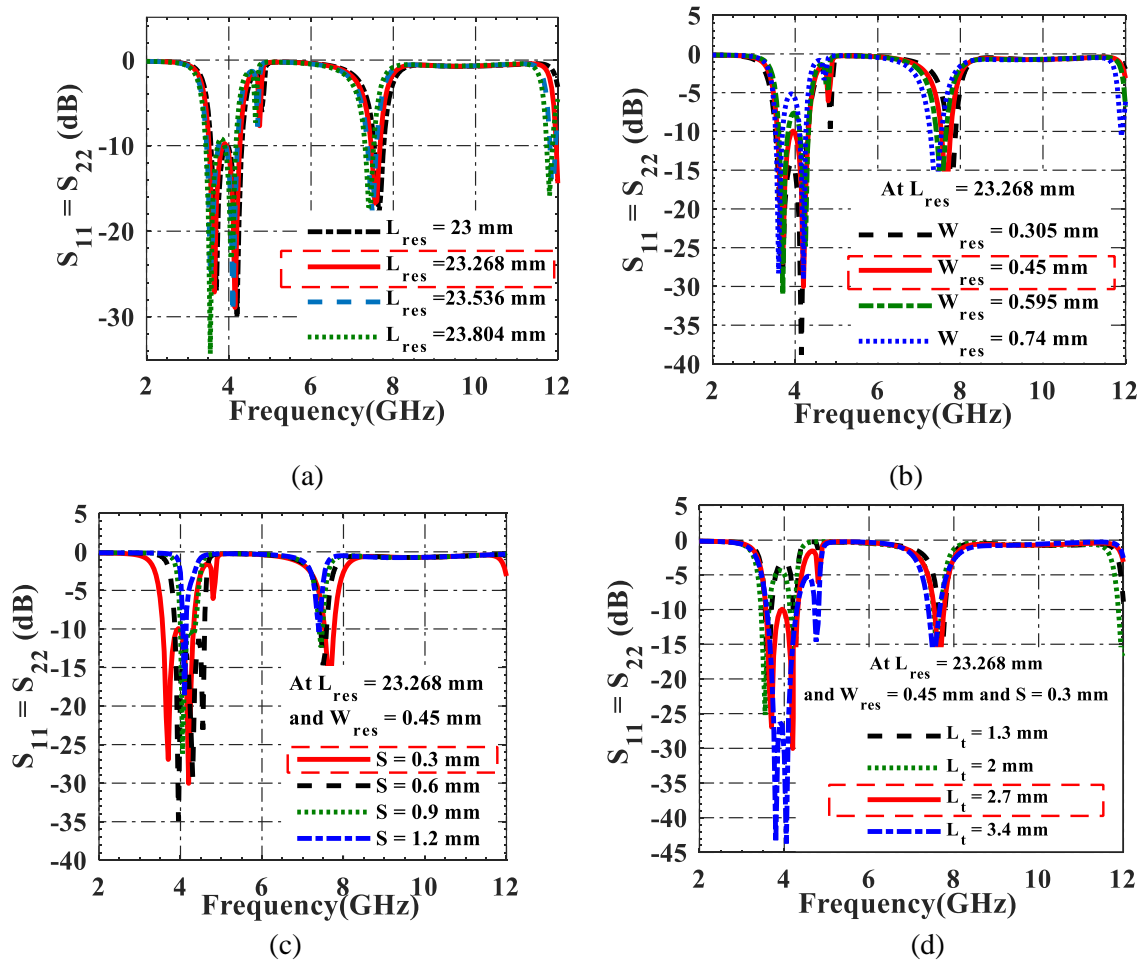


Figure 3. (a) Variation of mutual coupling due to the space between adjacent resonators and (b) Variation of external factor due to the tapping length of 3.95-GHz HPBF.



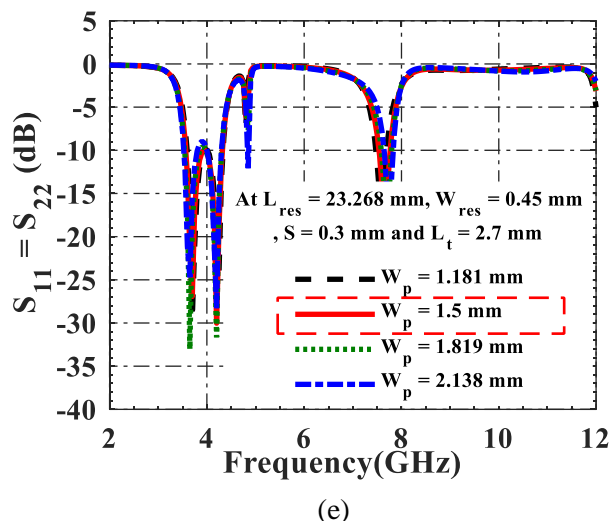


Figure 4. Parametric studies of the proposed 3.95 GHz HPBF on (a) L_{res} , (b) W_{res} , (c) S , (d) L_t and (e) W_p .

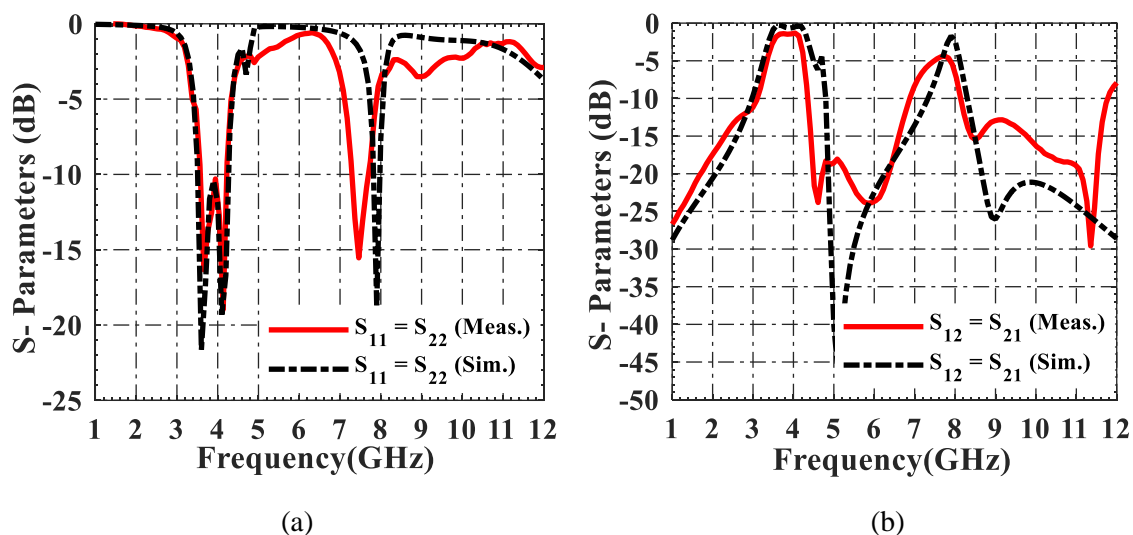


Figure 5. Simulated and measured (a) Return loss and (b) Insertion loss of the proposed 3.95-GHz HPBF.

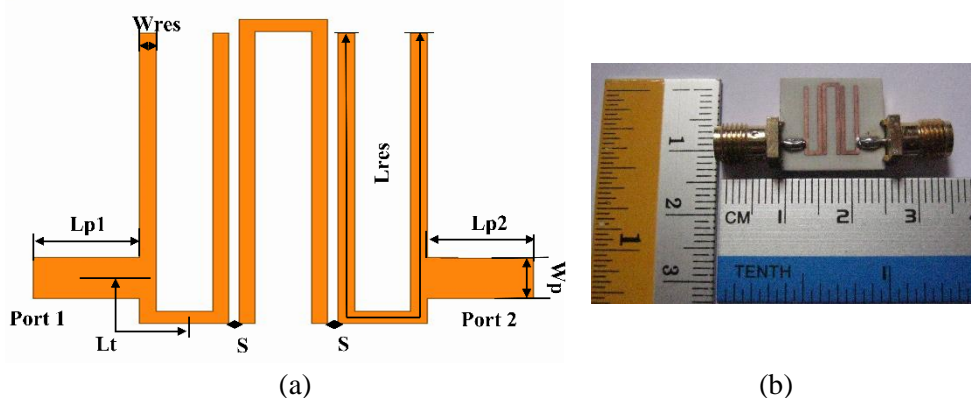


Figure 6. (a) Layout of the proposed 3.95 GHz HPBF and (b) fabricated prototype.

As shown in Figure 5a, good matching and transmitting response are obtained for the designed filter, where the measured and simulated return losses are less than -10 dB and -10.45 dB with enhanced BW of 0.1 GHz and 0.3 GHz through 3.57 GHz – 4.17 GHz and 3.45 GHz – 4.24 GHz, respectively. Also, the measured and simulated insertion losses are around -1.5 dB and -0.78 dB at centre frequencies $F_c = 3.75$ GHz and 3.81 GHz, respectively, as shown in Figure 5b. In addition, one can observe that the

proposed 3.95 GHz HPBF can support up to only 7.8 GHz (Sim.) and 8 GHz (Meas.) harmonics suppression. Because this harmonic will occur within the UWB, this filter is not preferable in reconfigurable 5G narrow band / UWB reconfigurable antenna applications, such as Cognitive Radios (CRs). To overcome this limitation, Defected Ground and Microstrip Structures (DGS) and (DMS) can be added to the filter as in [19]-[20] and [8], respectively. Moreover, another type of compact structure filter can be used, such as interdigital filter that supports high-order harmonics suppression [1]. The layout and the fabricated prototype of the designed filter are shown in Figure 6. The circuit area of this filter is 14.1 mm x 11.2 mm ($0.31 \lambda_g \times 0.24 \lambda_g$).

4. 6.55-GHz UNIFORM TRANSMISSION LINE HAIRPIN BANDPASS FILTER

Based on the design equations (1) - (4), 6.55 GHz HPBF is designed. Table 2 indicates all the calculated and optimized parameters of the filter. Figure 7 shows the variation of M_{12} and Q_e due to S and L_t , respectively. The optimized parameters in Table 2 are obtained *via* parametric studies to get better filter matching responses, as indicated in Figure 8. The optimized parameters in Figure 8 are in red solid line either a dashed red box. Figure 8a indicates that at the calculated L_{res} (14.324 mm), the band is shifted to the right and good matching within the required band is obtained when L_{res} increases a little bit to 15.524 mm. No matching is obtained when $W_{res} < 0.5$ mm, as shown in Figure 8b and although matching is good at $W_{res} = 0.7$ mm, the high frequency of the band is covered when $W_{res} = 0.6$ mm. Figure 8c illustrates that to increase the BW, the coupling between resonators should be increased by decreasing S and the best matching within the required frequency band is obtained at $S = 0.3$ mm. As shown in Figure 8d, good matching is obtained at $L_t = 2.9$ mm. The proposed HPBF is shown in Figure 9. The dimensions of this filter are 17.3 mm x 6.91 mm ($0.66 \lambda_g \times 0.27 \lambda_g$).

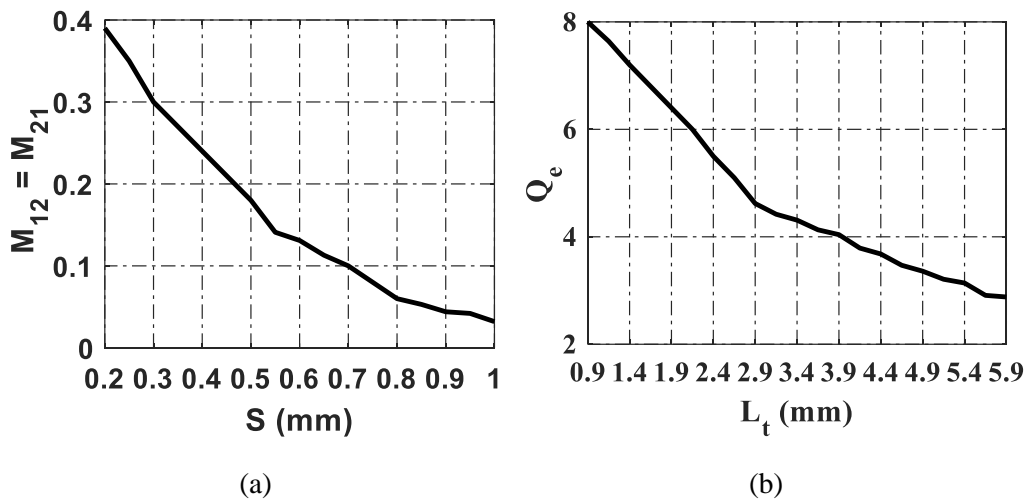


Figure 7. (a) Variation of mutual coupling due to the space between adjacent resonators and (b) Variation of an external factor due to the tapping length of 6.55 UTL HPBF.

Table 2. Calculated and optimized parameters for 6.55-GHz HPBF.

Parameters	Calculated	Optimized
Q_e	7.84	-
$M_{12}=M_{21}$	0.162	-
L_{res} (mm)	14.324	15.524
W_{res} (mm)	0.5	0.6
S (mm)	0.65	0.3
L_t (mm)	1.3	2.9
$L_{p1}=L_{p2}$ (mm)	-	4
W_p (mm)	1.819	1.819

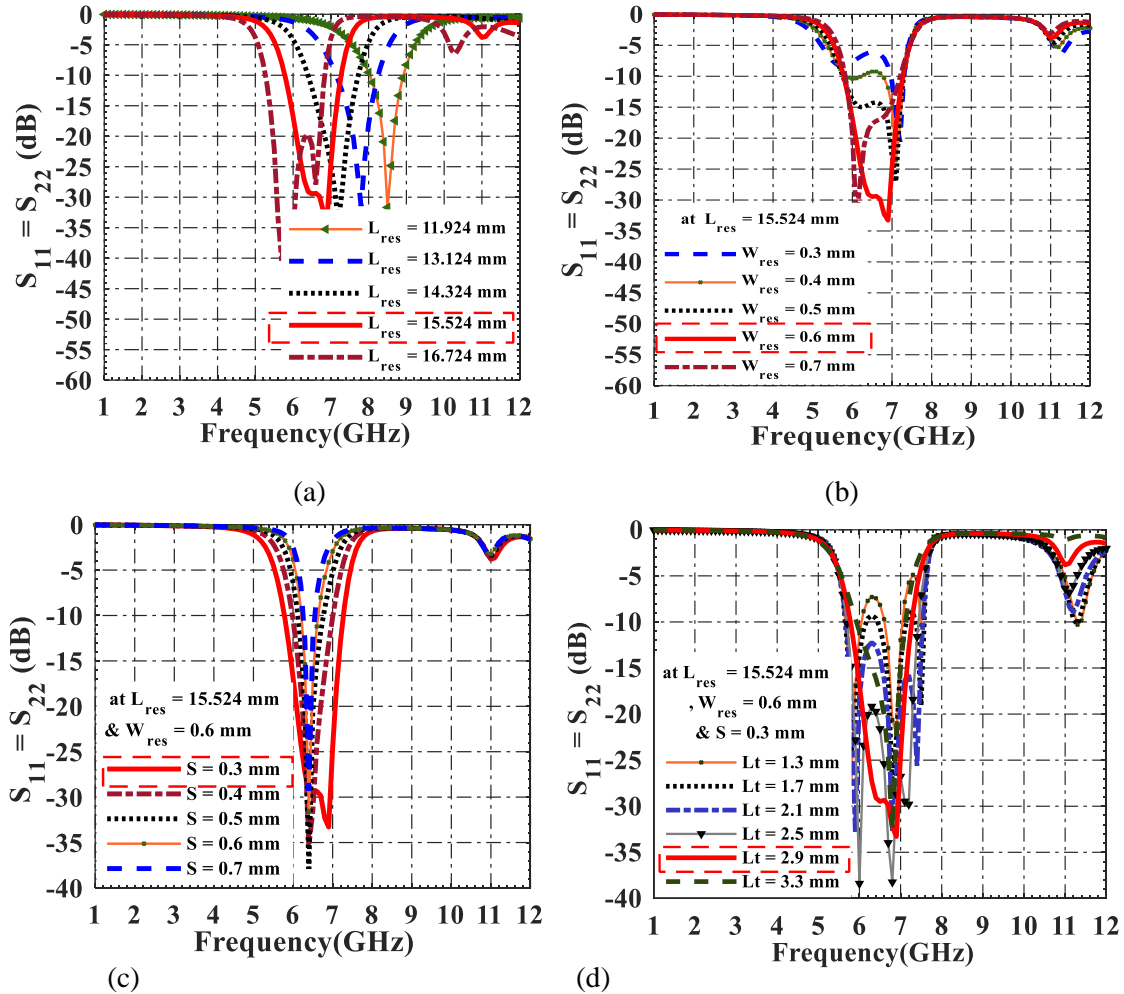


Figure 8. Parametric studies of the proposed 6.55 GHz UTL HPBF on (a) L_{res} , (b) W_{res} , (c) S and (d) L_t .

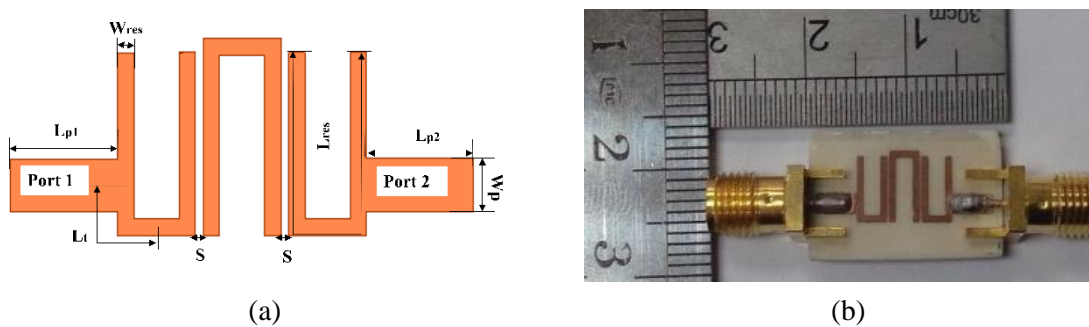


Figure 9. (a) Layout of the proposed 6.55-GHz HPBF and (b) Fabricated prototype.

Figure 10 illustrates the simulated and measured results for the designed 6.55-GHz HPBF with good impedance matching, transmission response and up to 11.1 GHz harmonics suppressions, where $S_{11} = S_{22}$ is < -11.66 dB (Meas.) and < -19 dB (Sim.) with a BW enhancement of 0.83 GHz and 0.33 GHz and up to 11 GHz at frequency ranges (5.62 GHz – 7.6 GHz) and (5.87 GHz – 7.35 GHz), respectively. However, $S_{12} = S_{21}$ is around -1.17 dB (Meas.) and -0.5 dB (Sim.) at center frequency 6.61 GHz. The difference between simulated and measured results is due to the fabrication and measurement tolerances. These good results make the filter suitable to be integrated into our 5G narrowband / UWB reconfigurable antenna project.

Finally, Table 3 shows a comparison of the proposed filters in this paper with other HPBFs in the literature with different frequency ranges. As it is clear from the table in terms of narrowband, the proposed 5G HPBF provides wider BW at the two frequency bands with good impedance matching and transmission response.

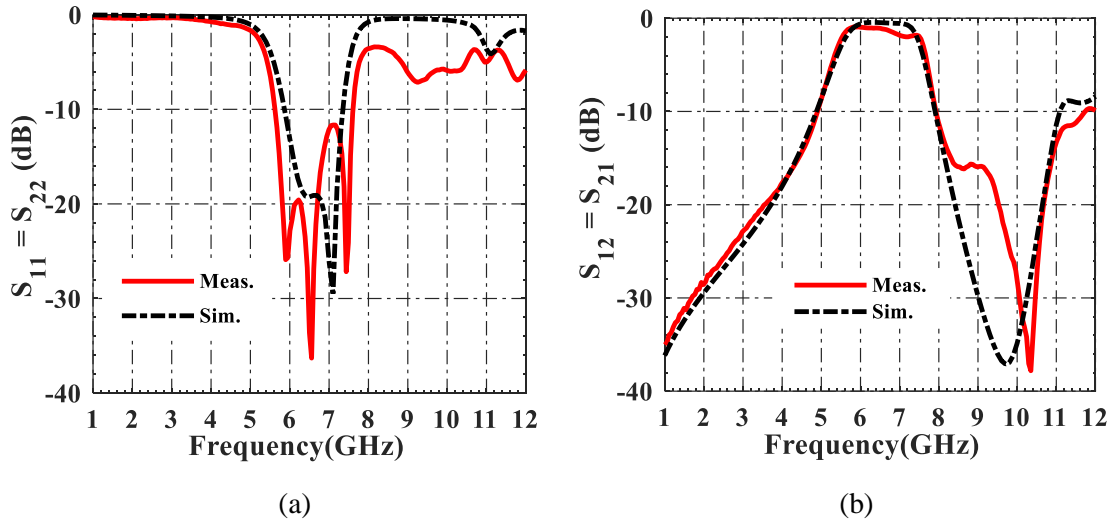


Figure 10. Simulated and measured (a) Return loss and (b) Insertion loss of the proposed 6.55-GHz HPBF.

Table 3. Comparison to other related works to HPBF in the literature for the last ten years.

Ref.	Technique used	Substrate h(mm)/ ϵ_r	F_C GHz	3 dB FBW, Freq. Band GHz	$S_{11}=S_{22}$ (dB)<	$S_{12}=S_{21}$ (dB)	Circuit area
This Work Single Layer	UTL	0.813/3.55	3.75	21.1% 3.45– 4.24	-10	-1.5	$0.31 \lambda_g \times 0.24 \lambda_g$
	UTL	0.813/3.55	6.61	30% 5.62– 7.6	-11.66	-1.17	$0.66 \lambda_g \times 0.27 \lambda_g$
[4] Single Layer	UTL	0.508/2.33	5.66	4.45% 5.608– 5.86	-23.9	-4.4	$0.97 \lambda_g \times 0.68 \lambda_g$
[14] Single Layer	UTLs via holes	1.52/2.2	0.92	0.004% 0.92–0.924	-18.9	-7.7	$0.32 \lambda_g \times 0.17 \lambda_g$
[26] Single Layer	FSLs	1.6/4.4	1	25% 0.875–1.125	-27	-1.37	$0.26 \lambda_g \times 0.2 \lambda_g$
[7] Single Layer	UTLs using IPT on LCP	0.1/3.2	30.4	15% 28.12 – 32.68	-18.9	2.41	$0.50 \lambda_g \times 0.48 \lambda_g$
[27] Multilayers	LHRHTLs by LCPT	different/ different	2.06	24% 1.813 – 2.307	-11	1.5	$11.8 \times 4.8 \text{ mm}^2$
[8] Single Layer	NCLs	0.127 /2.94	31.57	3.45% 31.02–32.11	-9	-3.5	$2.16 \lambda_g \times 0.25 \lambda_g$
[28] Multilayers	UTLs with apertures for coupling	1.27 /6.15	2.5	4.75% 2.44 –2.56	-11	-1.65	$0.42 \lambda_g \times 0.41 \lambda_g$
[20] Single Layer	UTLs with square DGS	1.6/4.4	3	20.72% 2.9 – 3.1	-46.64	-0.3	$0.23 \lambda_g \times 0.18 \lambda_g$
[29] Multilayers	Higher ϵ_r substrate	0.381/9.8	8	15% at 7.4 – 8.6	-14.5	-3	$0.48 \lambda_g \times 0.48 \lambda_g$
[22] Single Layer	UTLs with dumbbell and (SHPR) DGSs	1.524/3.48	2.4	29% 2 – 2.7	-26	-3	$0.65 \lambda_g \times 0.33 \lambda_g$
[19] Single Layer	UTLs with square DGS	0.348/1.524	2.92	97.33% 2.82 – 3.02	-19.5	-1.6	$0.87 \lambda_g \times 0.29 \lambda_g$
[9] Single Layer	UTLs with square DGS	1.58 /2.2	9.3	30.11% 9.11 – 9.39	-19.2	-3.7	$1.81 \lambda_g \times 0.35 \lambda_g$
[6] Single Layer	S.C. comb-lines with RSRL resonator	0.5 /2.55	2.45	0.4082% 2.4 –2.5	-36.71	-0.36	$0.26 \lambda_g \times 0.1 \lambda_g$
[30] Multilayers	UTLs using IPDT	different/different	95.5	0.83% 91.9 –99.9	-10	-5	$0.95 \times 0.4 \text{ mm}^2$

5. CONCLUSION

Two 5G low-frequency band (3.7 GHz - 4.2 GHz and 5.975 GHz - 7.125 GHz) Hairpin Bandpass Filters (HPBFs) suitable for filtering and reconfigurable antenna applications are designed and simulated in this work. At the two bands, the results are good in terms of return and insertion losses. A filter is fabricated and tested at both frequency bands. The measured S_{11} and S_{12} are < -10 dB and < -10.66 dB and -1.5 dB and -1.17 dB, through 3.45 GHz- 4.25 GHz and 5.62 GHz – 7.6 GHz, respectively. As

future work, many techniques can be used to reduce the size of this filter and to get further harmonics suppressions, especially at the first band (3.7 GHz – 4.2 GHz) to be compatible with 5G narrow band / UWB reconfigurable antenna.

ACKNOWLEDGEMENTS

This work was supported by the University of Science Malaysia through the RUI Grants (1001/PELECT/801405) and (304/PELECT/6315294).

REFERENCES

- [1] J.-S. G. Hong and M. J. Lancaster, *Microstrip Filters for RF/Microwave Applications*, vol. 167, John Wiley & Sons, 2011.
- [2] Q. Abdullah, N. S. M. Shah, N. Farah, W. A. Jabbar, N. Abdullah, A. Salh et al., "A Compact Size Microstrip Five Poles Hairpin Band-pass Filter Using Three-layers Structure for Ku-band Satellites Application," *Telkomnika*, vol. 18, no. 1, pp. 80-89, 2020.
- [3] K. K. Sethi, A. Dutta, G. Palai and P. Sarkar, "Hairpin Structure Band-pass Filter for IoT Band Application," *New Paradigm in Decision Science and Management, Part of the Advances in Intelligent Systems and Computing Book Series (AISC)*, vol. 1005, pp. 399-405, Springer, 2020.
- [4] N. A. Wahab, W. N. W. Muhamad, M. M. A. M. Hamzah, S. S. Sarnin and N. F. Naim, "Design A Microstrip Hairpin Band-pass Filter for 5GHz Unlicensed WiMAX," *Proc. of IEEE International Conference on Networking and Information Technology*, pp. 183-186, Manila, Philippines, 2010.
- [5] M. F. M. Yusoff, M. A. M. Sobri, F. Zubir and Z. Johari, "Multiband Hairpin-line Bandpass Filters by Using Metamaterial Complementary Split Ring Resonator," *Indonesian Journal of Electrical Engineering and Informatics (IJEI)*, vol. 7, pp. 289-294, 2019.
- [6] S. K. Azam, M. I. Ibrahimy, S. Motakabber, A. Z. Hossain, and M. S. Islam, "A miniaturized hairpin resonator for the high selectivity of WLAN bandwidth," *Bulletin of Electrical Engineering and Informatics*, vol. 8, pp. 916-922, 2019.
- [7] H.-I. Kao, C.-L. Cho, X. Dai, C.-S. Yeh, X.-Y. Zhang, L.-C. Chang et al., "Hairpin Bandpass Filter on Liquid Crystal Polymer Substrate Using Inkjet Printing Technology," *Proc. of IEEE MTT-S International Microwave Symposium Digest (MTT)*, pp. 1-4, Seattle, WA, USA, 2013.
- [8] H. Shaman, S. Almorqi, O. Haraz and S. Alshebeili, "Hairpin Microstrip Bandpass Filter for Millimeter-wave Applications," *Proceedings of IEEE Mediterranean Microwave Symposium (MMS2014)*, pp. 1-4, Marrakech, Morocco, 2014.
- [9] B. Adli, R. Mardiaty and Y. Y. Maulana, "Design of Microstrip Hairpin Bandpass Filter for X-band Radar Navigation," *Proc. of the IEEE 4th International Conference on Wireless and Telematics (ICWT)*, pp. 1-6, Nusa Dua, Indonesia, 2018.
- [10] K. Kavitha and M. Jayakumar, "Design and Performance Analysis of Hairpin Bandpass Filter for Satellite Applications," *Procedia-Computer Science*, vol. 143, pp. 886-891, 2018.
- [11] S. Ono and K. Wada, "Design and Fabrication of 3-Pole BPF Configured by Hairpin Resonators and Different Types of Coupling and Feed Types at 20 GHz," *Proc. of IEEE Asia-Pacific Microwave Conference (APMC)*, pp. 1363-1365, Kyoto, Japan, 2018.
- [12] M. Fadhil, H. Wijanto and Y. Wahyu, "Hairpin Line Bandpass Filter for 1.8 GHz FDD-LTE eNodeB Receiver," *Proc. of the International IEEE Conference on Radar, Antenna, Microwave, Electronics and Telecommunications (ICRAMET)*, pp. 134-136, Jakarta, Indonesia, 2017.
- [13] O. Sharifi-Tehrani, "Design, Simulation and Fabrication of Microstrip Hairpin and Interdigital BPF for 2.25 GHz Unlicensed Band," *Majlesi Journal of Telecommunication Devices*, vol. 6, pp. 115-118, 2017.
- [14] F. Y. Zulkifli, R. Saputra and E. T. Rahardjo, "Microstrip Hairpin Bandpass Filter Using Via Ground Holes for 923 MHz RFID Application," *Proc. of the International Symposium on Antennas and Propagation (ISAP)*, Jeju, pp. 1-4, [Online], Available: [https://www.ieice.org/cs/isap/ISAP_Archives/2011/pdf/\[FrD4-6\]20A14_1003.pdf](https://www.ieice.org/cs/isap/ISAP_Archives/2011/pdf/[FrD4-6]20A14_1003.pdf), 2011.
- [15] A. Lalbakhsh, A. A. L. Neyestanak and M. Naser-Moghaddasi, "Microstrip Hairpin Bandpass Filter Using Modified Minkowski Fractal Shape for Suppression of Second Harmonic," *IEICE Transactions on Electronics*, vol. 95, pp. 378-381, 2012.

- [16] M. Naser-Moghadasi, M. Alamolhoda and B. Rahmati, "Spurious Response Suppression in Hairpin Filter Using DMS Integrated in Filter Structure," *Prog. In Electromag. Research*, vol. 18, pp. 221-229, 2011.
- [17] K. Vidhya and T. Jayanthi, "Design of Microstrip Hairpin Band Pass Filter Using Defected Ground Structure and Open Stubs," *Proc. of the International Conference on Information and Electronics Engineering (IPCSIT)*, vol. 6, pp. 268-272, IACSIT Press, Singapore, 2011.
- [18] M. Othman, N. M. Zaid, M. A. Aziz and H. Sulaiman, "3 GHz Hairpin Filter with Defected Ground Structure (DGS) for Microwave Imaging Application," *Proc. of the IEEE International Conference on Computer, Communications and Control Technology (I4CT)*, pp. 411-414, Langkawi, Malaysia, 2014.
- [19] N. Ismail, T. S. Gunawan, T. Praludi and E. A. Hamidi, "Design of Microstrip Hairpin Bandpass Filter for 2.9 GHz–3.1 GHz S-band Radar with Defected Ground Structure," *Malaysian Journal of Fundamental and Applied Sciences*, vol. 14, pp. 448-455, 2018.
- [20] V. S. Kershaw, S. S. Bhadauria and G. S. Tomar, "Design of Microstrip Hairpin-line Bandpass Filter with Square Shape Defected Ground Structure," *Asia-Pacific Journal of Advanced Research in Electrical and Electronics Engineering*, vol. 1, pp. 21-30, 2017.
- [21] T. Hariyadi and S. Mulyasari, "Design and Simulation of Microstrip Hairpin Bandpass Filter with Open Stub and Defected Ground Structure (DGS) at X-Band Frequency," *Proc. of the 2nd International Conference on Innovation in Engineering and Vocational Education, IOP Conference Series: Materials Science and Engineering*, vol. 306, p. 012124, Manado, Indonesia, 2018.
- [22] H. Sajjad, A. Altaf, S. Khan and L. Jan, "A Compact Hairpin Filter with Stepped Hairpin Defected Ground Structure," *Proc. of the 21st IEEE International Multi-topic Conference (INMIC)*, pp. 1-5, Karachi, Pakistan, 2018.
- [23] N. Ismail, S. M. Ulfah, I. Lindra, A. S. Awalluddin, I. Nuraida and M. A. Ramdhani, "Microstrip Hairpin Bandpass Filter for Radar S-Band with Dumbbell-DGS," *Proc. of the 5th IEEE International Conference on Wireless Communications and Telematics (ICWT)*, pp. 1-4, Yogyakarta, Indonesia, 2019.
- [24] J. Ye, D. Qu, X. Zhong and Y. Zhou, "Design of X-band Bandpass Filter Using Hairpin Resonators and Tapped Feeding Line," *Proc. of IEEE Symposium on Computer Applications and Communications*, pp. 93-95, Weihai, China, 2014.
- [25] T. Singh, J. Chacko, N. Sebastian, R. Thoppilan, A. Kotrashetti and S. Mande, "Design and Optimization of Microstrip Hairpin-line Bandpass Filter Using DOE Methodology," *Proc. of the IEEE International Conference on Communication, Information & Computing Technology (ICCICT)*, pp. 1-6, Mumbai, India, 2012.
- [26] A. Lotfi-Neyestanak and A. Lalbakhsh, "Improved Microstrip Hairpin-line Bandpass Filters for Spurious Response Suppression," *Electronics Letters*, vol. 48, pp. 858-859, 2012.
- [27] J. Ni, "Development of Tunable and Miniature Microwave Filters for Modern Wireless Communications," *Heriot-Watt University*, [Online], Available: <http://hdl.handle.net/10399/2843>, 2014.
- [28] N. Chami, D. Saigaa, A. Djaiz, R. AlThomali and M. Nedil, "A New Miniature Microstrip Two-layer Bandpass Filter Using Aperture-coupled Hairpin Resonators," *International Journal of Advanced and Applied Sciences*, vol. 4, pp. 10-14, 2017.
- [29] M. Tan, Y. Xuan, Y. Ma, L. Li and Y. Zhuang, "Design of C-band Interdigital Filter and Compact C-band Hairpin Bandpass Film Filter on Thin Film Substrate," *RF and Microwave Microelectronics Packaging II*, pp. 63-73, Springer, 2017.
- [30] B. Chen, Y. Tang, H. Zhu, H. Yue, Z. Wen and X. Deng, "Design of W Band Hairpin Filter with IPD Technology," *Proc. of IEEE MTT-S International Wireless Symposium (IWS)*, pp. 1-3, Guangzhou, China, 2019.
- [31] C. Schuster, A. Wiens, M. Schübler, C. Kohler, J. Binder and R. Jakoby, "Hairpin Bandpass Filter with Tunable Center Frequency and Tunable Bandwidth Based on Screen Printed Ferroelectric Varactors," *Proc. of the 46th IEEE European Microwave Conference (EuMC)*, pp. 1425-1428, London, UK, 2016.
- [32] C. Schuster, L. Schynol, E. Polat, E. Schwab, S. Schmidt, R. Jakoby et al., "Reconfigurable Hairpin Filter with Tunable Center Frequency, Bandwidth and Transmission Zero," *Proc. of the IEEE MTT-S International Microwave Workshop Series on Advanced Materials and Processes for RF and THz Applications (IMWS-AMP)*, pp. 79-81, Bochum, Germany, 2019.
- [33] M. A. Almahadeen and A. M. Matarneh, "Performance Assessment of Throughput in a 5G System," *Jordanian Journal of Computers and Information Technology (JJCIT)*, vol. 6, no. 3, pp. 303-316, 2020.

- [34] M. A. Taher, "Enhanced 5G Throughput Using UFMC Multiplexing," Journal of Southwest Jiaotong University, vol. 54, no. 5, pp. 1-11, 2019.
- [35] I. Parvez, A. Rahmati, I. Guvenc, A. I. Sarwat and H. Dai, "A Survey on Low Latency Towards 5G: RAN, Core Network and Caching Solutions," IEEE Communications Surveys & Tutorials, vol. 20, pp. 3098-3130, 2018.
- [36] J. Sachs, G. Wikstrom, T. Dudda, R. Baldemair and K. Kittichokechai, "5G Radio Network Design for Ultra-reliable Low-latency Communication," IEEE Network, vol. 32, pp. 24-31, 2018.
- [37] O. N. Yilmaz, Y.-P. E. Wang, N. A. Johansson, N. Brahmi, S. A. Ashraf and J. Sachs, "Analysis of Ultra-reliable and Low-latency 5G Communication for a Factory Automation Use Case," Proc. of the IEEE International Conference on Communication Workshop (ICCW), pp. 1190-1195, London, UK, 2015.
- [38] R. Pawlak, P. Krawiec and J. Żurek, "On Measuring Electromagnetic Fields in 5G Technology," IEEE Access, vol. 7, pp. 29826-29835, 2019.
- [39] 5G Americas, "5G Spectrum Vision," 5G Americas White Paper, p. 50, [Online], Available: <https://www.5gamericas.org/5g-spectrum-vision/>, February 2019.
- [40] S. Saleh, W. Ismail, I. S. Z. Abidin and M. H. Jamaluddin, "N-way Compact Ultra-wide Band Equal and Unequal Split Tapered Transmission Lines Wilkinson Power Divider," Jordanian Journal of Computers and Information Technology (JJCIT), vol. 6, no. 3, pp. 291-302, September, 2020.
- [41] Em:Talk, "Microstrip Line Calculator," [Online], Available: <http://www.emtalk.com/mscalc.php>.
- [42] D. M. Pozar, Microwave Engineering, Hoboken, NJ: John Wiley & Sons, 2012.

ملخص البحث:

في هذه الورقة، يتم تصميم ومحاكاة وتصنيع مرشح تمرير نطاق ترددي على شكل مُعطَف عند نطاقين تردديين منخفضين: (3.7-4.2 جيجا هيرتز، و 5.975-7.125 جيجا هيرتز). وهذا المرشح سيكون جزءاً من مشروع الهوائيات المنتمي الى الجيل الخامس الذي نعمل عليه، والقابل لإعادة التشكيل لكل من النطاقات الضيقة/ النطاقات فائقة العرض (UWB/NB)، والذي من شأنه أن يلعب دوراً أساسياً في الشبكات اللاسلكية الحديثة؛ مثل شبكات الراديو الإدراكي (CRs) وعلى مدى النطاقين التردديين، حصلنا من المرشح على مواعمة واستجابة إرسال جيدتين، مع عرض نطاق محسّن. وبلغ معامل الانعكاس المقاس للمرشح المقترح أقل من (-10) ديسيبل وأقل من (11.66) ديسيبل على مدى النطاقين التردديين (3.45-4.25 جيجا هيرتز، و 5.62-7.6 جيجا هيرتز) على الترتيب. أما معامل الإرسال فكان في حدود (-1.5) ديسيبل، و (-1.17) ديسيبل عند الترددات المركزيين (3.75 جيجا هيرتز، و 6.61 جيجا هيرتز على التوالي. وفي هذا البحث، استخدمت برمجية المحاكاة البنيوية للترددات العالية (HFSS) لإجراء المحاكاة. وقد تم التحقق من نتائج المحاكاة للموجة الكاملة، مع القياسات المرتبطة بالمعدات.

